

Thermal, Mechanic, and Magnetic Properties of Ni₅₄Mn₁₈Ga₂₀Fe₈ Magnetic Shape Memory Alloy

Alim Bozer, Erdem Yaşar

Department of Physics, Kırıkkale University, Kırıkkale, Turkey

ABSTRACT

This paper represents some new experimental results about thermal, mechanical and magnetic properties in NiMnGaFe ferromagnetic shape memory alloy. Ni₅₄Mn₁₈Ga₂₀Fe₈ polycrystalline shape memory alloy was fabricated by an arc melting device providing inert argon gas atmosphere. Martensitic transformation (MT) temperatures of Ni₅₄Mn₁₈Ga₂₀Fe₈ alloy were determined by DSC and the crystal structure of alloy was investigated by XRD. Shape memory effect of alloy was determined by TMA and after the necessary calculations are made, the results are found as the residual strain $\epsilon_r = 3$, shape memory effect $\epsilon_{SME} = 2.6$ and the recovery rate = 86.6%. The magnetic properties were determined using Mossbauer spectroscopy. The magnetic properties were determined using Mossbauer spectra. The results demonstrated that the presence of two phases coexist which are gamma phase and martensitic phase.

Keywords: Martensitic Phase Transformation, Mossbauer, SEM, Shape Memory Alloy, XRD.

Date of Submission: 26-09-2017

Date of Accepted: 06-10-2017

I. INTRODUCTION

Technological studies require the production of materials suitable for the purpose of use. In this context, intensive studies have been made on NiMnGa alloys and these alloys continue to be investigated. The aim of the researches is to increase the quality and usage areas of the alloys with various chemical and physical effects. Along with many of the features found, the study of these alloys still requires the discovery of new features. From the beginning of 2000s, NiMnGa ternary ferromagnetic shape memory alloys (FSMAs) have attracted a huge interest since they have some unique features compared to other smart materials some of which are response to an applied magnetic field and quick response time to it [1-6]. On closer inspection of ferromagnetic shape memory alloy class, the largest magnetic induced strains under a magnetic field have been observed in NiMnGa ternary alloy systems with different element ratios [1]. This observed large strains have made NiMnGa FSMAs as a potential candidate of smart material for developing new kind of actuators that can produce a large displacement [7].

Unfortunately, the NiMnGa ternary alloy systems have some problems in terms of using them in industrial applications some of these drawbacks are; magnetic output power, low Curie temperature, brittleness and ductility. Having studied the literature, it can be found that the addition of some elements may enhance some of disadvantages. Investigations to improve the easy breakage of NiMnGa-based alloys continue at full speed. Up to this point, it has been shown that tackling the brittleness properties of these alloys is possible either by increasing the Ni content in the alloy or making the alloy quaternary by adding an extra element such as Fe, Cu and Co [8-12]. It was found that Fe addition reinforced the toughness and brittleness of the NiMnGa alloy preserving the characteristics such as magnetic and thermoplastic properties [13]. However, few works have been made to declare the magnetic properties of Fe added NiMnGa quaternary alloys with other works at the same time including shape memory effect and magnetic, thermal and mechanical properties. This study seeks for some answers about a wide range of properties of Ni₅₄Mn₁₈Ga₂₀Fe₈ ferromagnetic shape memory alloy, and in this way it is also aimed to make some useful contribution to shape memory alloy field.

II. EXPERIMENTAL

In order to produce a high purity alloy, elements constituting the alloy (Nickel 99.98%, Manganese 99.9%, Gallium 99.9% and Iron 99.9%) were remelted in an Arc Melter for five times in an inert argon gas atmosphere to reach desired high homogeneity target, after this consecutive melting procedure alloy was remelted in a different copper mold for the last time to get Ni₅₄Mn₁₈Ga₂₀Fe₈ ingot with diameter 3 mm and length 70 mm. The alloy was taken into a quartz tube, thereafter homogenization process was performed at 900 °C for 22 hours

in a high temperature furnace and then quenched into ice water which is pre-prepared. After quenching, the heat treated alloy was cut with the slow speed diamond saw to get some slices in preparation for analyzes. Sample for SEM observations was mechanically polished using different thickness sandpaper and then chemically etching procedure was performed in a chemical mixture including 99 ml methanol, 2 ml nitric acid and 5 g ferric chloride. The chemical composition of produced alloy was determined by Energy Dispersive X-ray (EDX) analysis, which is equipped in SEM, averaged from five data points. Sample for compression and thermomechanical analysis was cut from the quenched alloy with 5 mm length (diameter was 3 mm). Thermomechanical analysis was performed on a Thermomechanical Analyzer (TMA SDTA 841, Mettler Toledo) heating and cooling rate of 10 °C min⁻¹ and the temperature scale for thermomechanical analysis was between 30 °C and 600 °C. Before thermomechanical analysis, the sample was compressed by 6% using Shimadzu EHF-LV005K2-010 and crosshead speed was chosen as 0.2 mm/min, and then compressed sample was put into TMA to perform thermomechanical cycle from room temperature to 600 °C. In order to identify phase structure of alloy is either single or dual, X-ray diffraction (XRD, Bruker D8 advance) measurement was taken with Cu K α radiation on powder sample at room temperature at the range of 20°-100° with the scanning rate of 1°/min. The phase transformation temperatures, which are Ms, Mf, Mp, As, Af and Ap, of alloy were determined by DSC (DSC1, Mettler Toledo) using nitrogen gas at the heating and cooling speed of 10 °C/min. The Mossbauer spectroscopy measurement of grinded alloy was measured at room temperature. ⁵⁷Co-Rh source with an activity of 50mCi was used in Mossbauer spectra measurement. Calibration of speed scale was provided by α -Fe. Fitting procedure of the obtained spectra was made by a fit program called Win Normos.

III. RESULTS

3.1 Microstructure Analysis

Fig. 1 shows the SEM analysis result of Ni₅₄Mn₁₈Ga₂₀Fe₈ alloy after annealing and etching procedure were done. It can be seen from Fig. 1 that the polycrystalline alloy is composed of two-phase, martensite given by the letter of M and gamma phase given by the symbol of γ . The result is compatible that two phase microstructure consist of martensite and γ phase have reported earlier by other authors [9]. The microstructure of martensite phase has been observed as layered form, and fine layers, martensite twins and grain boundaries can be seen clearly from Fig. 1. Fig. 2 shows XRD result of Ni₅₄Mn₁₈Ga₂₀Fe₈ alloy. XRD method is a useful method to determine the crystal structure of alloys, in this study XRD measurement is performed at room temperature (from $2\theta = 20$ to $2\theta = 100$ and the scanning rate was chosen as 1°/min). The results showed that martensite and austenite peaks coexist, which is consistent with the SEM results given in Fig. 1. Typical martensite peaks can be seen easily from Fig. 2, the crystal lattice parameters of the martensitic phase is found as a tetragonal type and the second phase is the face-centered cubic γ phase.

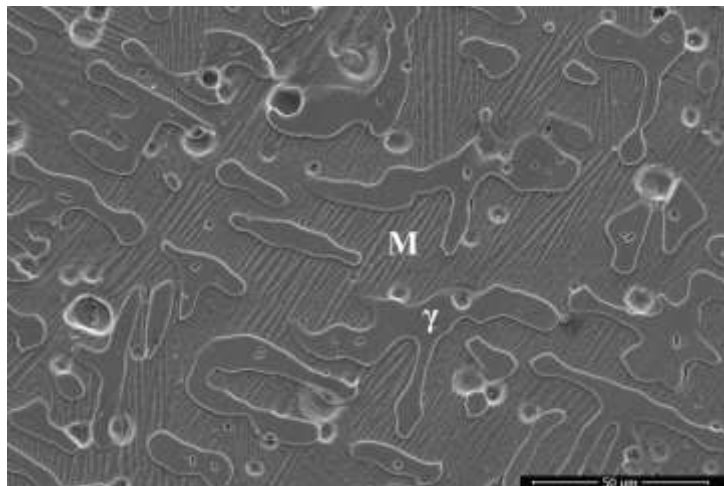


Figure 1. Microstructure of Ni₅₄Mn₁₈Ga₂₀Fe₈ alloy.

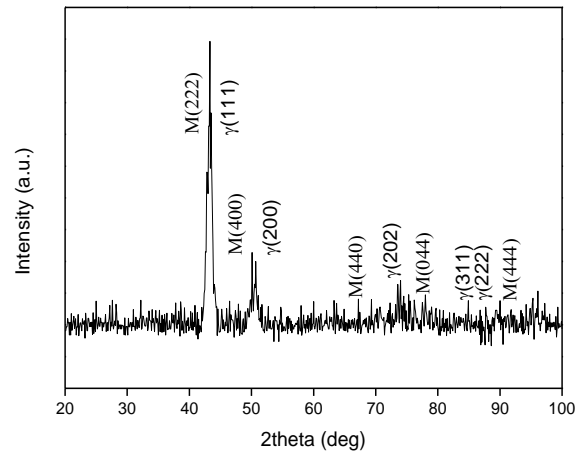


Figure 2. X-ray diffraction pattern.

Differential scanning calorimeter (DSC) curve of Ni₅₄Mn₁₈Ga₂₀Fe₈ alloy is shown in Fig. 3. DSC peaks measured during heating and cooling revealed the MT temperature of alloy. Martensite start and finish (Ms, Mf) and austenite start and finish (As, Af) temperatures were determined by a practical method which is known as tangent intersection method in DSC analysis. Start and finish transformation temperatures (Ms, Mf, As, Af) of Ni₅₄Mn₁₈Ga₂₀Fe₈ alloy are found as 219.79, 207.04, 262.2, 286.44 °C, respectively.

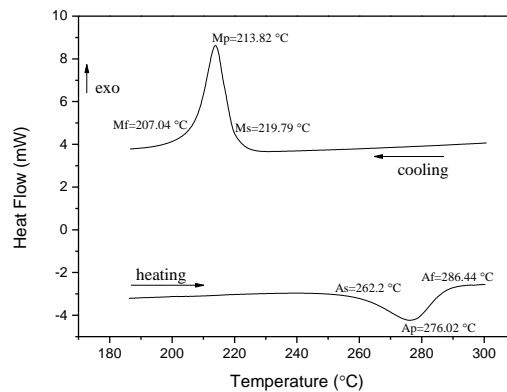


Figure 3. DSC curves of Ni₅₄Mn₁₈Ga₂₀Fe₈ alloy at a temperature rate of 10 °C/min.

3.2 Shape Memory Effect

Shape memory effect (SME) of Ni₅₄Mn₁₈Ga₂₀Fe₈ alloy is determined by two sequential processes. Before the TMA test, cylindrical sample (diameter 3 mm and length 5 mm) is compressed in static test at room temperature as given in Fig. 4. Static test result showed that alloy is broken at 8% strain. This test was made to determine how much strain is suitable to have been carried out. After compression test it was decided that 6% strain is enough to check shape memory effect.

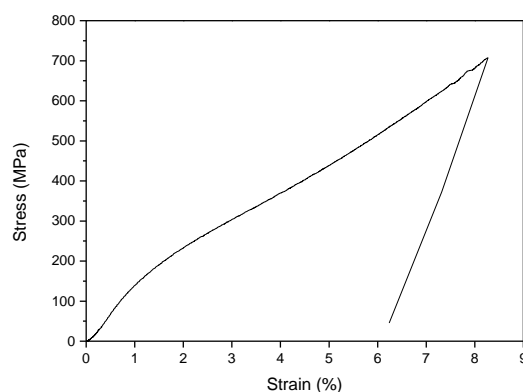


Figure 4. The compressive stress-strain curve of $\text{Ni}_{54}\text{Mn}_{18}\text{Ga}_{20}\text{Fe}_8$ alloy at room temperature.

Cylindrical sample ($\text{Ø}3 \text{ mm} \times 5 \text{ mm}$) that was cut from the same ingot strained 6% and then one thermomechanical cycling was performed as in Fig. 5. The temperature range for thermomechanical cycling was from $25 \text{ }^\circ\text{C}$ to $600 \text{ }^\circ\text{C}$ and from $600 \text{ }^\circ\text{C}$ to $25 \text{ }^\circ\text{C}$ consecutively. The SME was calculated using the dimensional change of alloy before heating and after reverse transformation after the removal of length change due to thermal expansion as shown in Fig. 5. The details of the calculation are as follows: the length of sample was measured before loading (10), after unloading (11) and after thermomechanical cycling (12). The residual strain after unloading (ϵ_r) and the SME were calculated as $\epsilon_r = (10-11)/10 \times 100\%$, and $\epsilon_{\text{SME}} = (12-11)/10 \times 100\%$, respectively. The recoverable rates were calculated as: $R = \epsilon_{\text{SME}}/\epsilon_r$ [14]. After the necessary calculations are made, the results are found as $\epsilon_r = 3$, $\epsilon_{\text{SME}} = 2.6$ and the recoverable rate of 86.6%.

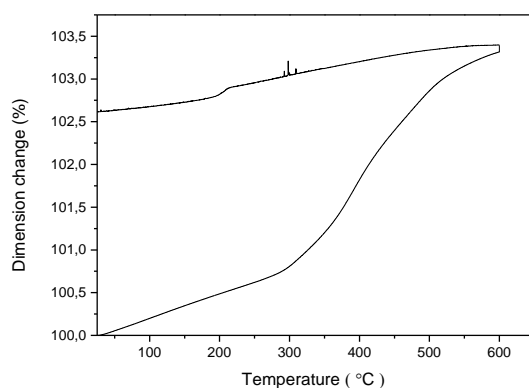


Figure 5. TMA curve of $\text{Ni}_{54}\text{Mn}_{18}\text{Ga}_{20}\text{Fe}_8$ alloy during thermomechanical cycle.

3.3. Mossbauer Results

Mossbauer spectroscopy is used to determine the concepts that the transitions between the energy levels in the core, the energy widths of the excited levels and their lifetimes, the core electric quadrupole moments, and the core magnetic dipole moments, the symmetry of the surrounding atoms or atom groups and hyperfine magnetic splitting (Zeeman effect). In this study Mossbauer spectroscopy is used to determine the local ordering, the magnetic moments and the magnetization orientation in Fe containing $\text{Ni}_{54}\text{Mn}_{18}\text{Ga}_{20}\text{Fe}_8$ alloy. Mossbauer spectroscopy is a well-known technique that can determine some parameters such as isomeric shift, internal magnetic splitting and quadruple splitting in Fe containing alloys.

In order to investigate Mossbauer spectra of $\text{Ni}_{54}\text{Mn}_{18}\text{Ga}_{20}\text{Fe}_8$ quaternary alloy, which had a bulk rod form before, was grinded firstly. Average particle size, which was found as 148.6 nm, was measured by Zetasizer. Then the powder sample is set for Mossbauer spectra. The ^{57}Fe Mossbauer spectra and fitted curves are shown in Fig. 6.

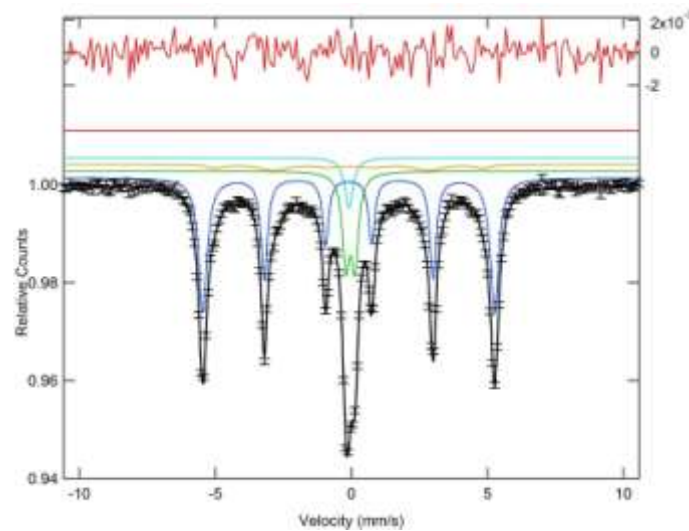


Figure 6. Mossbauer spectra of Ni₅₄Mn₁₈Ga₂₀Fe₈ alloy

Three essential interactions may be observed during Mossbauer measurements these are Isomeric shift (I.S) which is a chemical shift, quadruple splitting (Q.S) which splits a state into two, producing a doublet in the Mossbauer spectrum and Hyperfine magnetic splitting (Hhf) also known as Zeeman effect that leads to different effects such as shifts or splitting in the energy levels of atoms. Isomeric shifts of the alloy, volume ratios of internal phase structures and magnetic orientations of the austenite and martensite structures are presented by Mossbauer spectra in Fig. 6. Measured values are given in TABLE 1. For the ferromagnetism state, the sum of sextet 1 and sextet 2 is 75.989%, while the sum of singlet and doublet is found 24.011% which means paramagnetic structure.

Table 1. Parameters of Mossbauer Spectra of Ni₅₄Mn₁₈Ga₂₀Fe₈ alloy (Hhf : hyperfine magnetic field, I.S: isomer shift, Q.S: quadrupole splitting, W: line width, RA: Relative area)

Spectral Component	I.S. (mm s ⁻¹) (±0.003)	Q.S. (mms ⁻¹) (±0.005)	Hhf (T) (±0.03)	Volume (%)
Sextet 1	0.0061	0.0033	33.226	52.489
Sextet 2	0.0624	-0.0592	30.48	23.5
Doublet	0.071	0.3309	-	17.478
Singlet	0.0157	-	-	6.5322

IV. CONCLUSION

The present study reveals that the Ni₅₄Mn₁₈Ga₂₀Fe₈ alloy has good shape memory effect with the recoverable rates of 86.6%. Phase characteristics are determined DSC, SEM and Mossbauer results which are consistent with each other that all confirms alloy has two-phase together at the same time. It is noteworthy that the SME behaviors of two-phase Ni₅₄Mn₁₈Ga₂₀Fe₈ alloy has no similarity from those of other high temperature shape memory alloys [15, 16]. Influence of Fe addition on martensitic transformation temperatures is investigated and found that the addition of Fe element is increased the martensitic transformation temperature compared to previous studies made by some other researchers [17, 18].

ACKNOWLEDGEMENTS

We gratefully acknowledge the financial support for this study, provided by Kırıkkale University Scientific Research Projects Coordination Unit. Project Number: 2015/038.

REFERENCES

- [1] K. Ullakko, J. Huang, C. Kantner, R. O'handley, and V. Kokorin, "Large magnetic-field-induced strains in Ni₂MnGa single crystals," *Applied Physics Letters*, vol. 69, pp. 1966-1968, 1996.
- [2] Y. Long, Z. Zhang, D. Wen, G. Wu, R. Ye, Y. Chang, et al., "Phase transition processes and magnetocaloric effects in the Heusler alloys NiMnGa with concurrence of magnetic and structural phase transition," ed: AIP, 2005.
- [3] S. J. Murray, M. Marioni, S. Allen, R. O'handley, and T. A. Lograsso, "6% magnetic-field-induced strain by twin-boundary motion in ferromagnetic Ni-Mn-Ga," *Applied Physics Letters*, vol. 77, pp. 886-888, 2000.

- [4] Y. Liang, Y. Sutou, T. Wada, C.-C. Lee, M. Taya, and T. Mori, "Magnetic field-induced reversible actuation using ferromagnetic shape memory alloys," *Scripta Materialia*, vol. 48, pp. 1415-1419, 2003.
- [5] L. Ma, H. Zhang, S. Yu, Z. Zhu, J. Chen, G. Wu, et al., "Magnetic-field-induced martensitic transformation in MnNiGa: Co alloys," *Applied Physics Letters*, vol. 92, p. 032509, 2008.
- [6] L. Hirsinger and C. Lexcellent, "Internal variable model for magneto-mechanical behaviour of ferromagnetic shape memory alloys Ni-Mn-Ga," in *Journal de Physique IV (Proceedings)*, 2003, pp. 977-980.
- [7] J. Tellinen, I. Suorsa, A. Jääskeläinen, I. Aaltio, and K. Ullakko, "Basic properties of magnetic shape memory actuators," in 8th international conference ACTUATOR, 2002, pp. 566-569.
- [8] Y. Ma, C. Jiang, Y. Li, H. Xu, C. Wang, and X. Liu, "Study of Ni_{50+x}Mn₂₅Ga_{25-x} (x= 2-11) as high-temperature shape-memory alloys," *Acta materialia*, vol. 55, pp. 1533-1541, 2007.
- [9] Y. Q. Ma, S. Y. Yang, Y. Liu, and X. J. Liu, "The ductility and shape-memory properties of Ni-Mn-Co-Ga high-temperature shape-memory alloys," *Acta Materialia*, vol. 57, pp. 3232-3241, Jun 2009.
- [10] V. Sanchez-Alarcos, J. I. Perez-Landazabal, V. Recarte, C. Gomez-Polo, and J. A. Rodriguez-Velamazán, "Correlation between composition and phase transformation temperatures in Ni-Mn-Ga-Co ferromagnetic shape memory alloys," *Acta Materialia*, vol. 56, pp. 5370-5376, Nov 2008.
- [11] X. Q. Chen, X. Lu, D. Y. Wang, and Z. X. Qin, "The effect of Co-doping on martensitic transformation temperatures in Ni-Mn-Ga Heusler alloys," *Smart Materials & Structures*, vol. 17, Dec 2008.
- [12] I. Glavatskiy, N. Glavatska, A. Dobrinsky, J. U. Hoffmann, O. Sorberg, and S. P. Hannula, "Crystal structure and high-temperature magnetoplasticity in the new Ni-Mn-Ga-Cu magnetic shape memory alloys," *Scripta Materialia*, vol. 56, pp. 565-568, Apr 2007.
- [13] A. Cherechukin, I. Dikshtein, D. Ermakov, A. Glebov, V. Koledov, D. Kosolapov, et al., "Shape memory effect due to magnetic field-induced thermoelastic martensitic transformation in polycrystalline Ni-Mn-Fe-Ga alloy," *Physics Letters A*, vol. 291, pp. 175-183, 2001.
- [14] S. Yang, Y. Liu, C. Wang, Z. Shi, and X. Liu, "The mechanism clarification of Ni-Mn-Fe-Ga alloys with excellent and stable functional properties," *Journal of Alloys and Compounds*, vol. 560, pp. 84-91, 2013.
- [15] G. Firstov, J. Van Humbeeck, and Y. N. Koval, "High-temperature shape memory alloys: some recent developments," *Materials Science and Engineering: A*, vol. 378, pp. 2-10, 2004.
- [16] G. Firstov, J. Van Humbeeck, and Y. N. Koval, "Comparison of high temperature shape memory behaviour for ZrCu-based, Ti-Ni-Zr and Ti-Ni-Hf alloys," *Scripta materialia*, vol. 50, pp. 243-248, 2004.
- [17] C. Picornell, J. Pons, E. Cesari, and J. Dutkiewicz, "Thermal characteristics of Ni-Fe-Ga-Mn and Ni-Fe-Ga-Co ferromagnetic shape memory alloys," *Intermetallics*, vol. 16, pp. 751-757, 2008.
- [18] R. Singh, M. M. Raja, R. Mathur, and M. Shamsuddin, "Effect of Fe substitution on the phase stability and magnetic properties of Mn-rich Ni-Mn-Ga ferromagnetic shape memory alloys," *Journal of Magnetism and Magnetic Materials*, vol. 323, pp. 574-578, 2011.

Alim Bozer "Thermal, Mechanic, and Magnetic Properties of Ni₅₄Mn₁₈Ga₂₀Fe₈ Magnetic Shape Memory Alloy." *The International Journal of Engineering and Science (IJES)*, vol. 6, no. 9, 2017, pp. 68-73.